Measurement of the Branching Ratio for the $\Xi^- \to \Sigma^-\gamma$ Radiative Decay

T. Dubbs,[6,*] I. F. Albuquerque,[12] N. F. Bondar,[2] R. Carrigan, Jr.,[1] D. Chen,[8,†] P. S. Cooper,[1] Dai Lisheng,[3] A. S. Denisov,[2] A. V. Dobrovolsky,[2] A. M. F. Endler,[10] C. O. Escobar,[12] M. Foucher,[13,‡] V. L. Golovtsov,[2] H. Gottschalk,[1] P. Gouffon,[12] V. T. Grachev,[2] A. V. Khanzadeev,[2] M. A. Kubantsev,[7] N. P. Kuropatkin,[2] J. Lach,[1] Lang Pengfei,[3] Li Chengze,[3] Li Yunshan,[3] M. Luksys,[9,§] J. R. P. Mahon,[12] E. McCliment,[6] A. Morelos,[1,‖] C. Newsom,[6] M. C. Pommot Maia,[11,¶] V. M. Samsonov,[2] V. A Schegelsky,[2] Shi Huanzhang,[3] V. J. Smith,[4] Tang Fukun,[3] N. K. Terentyev,[2] S. Timm,[5] I. I. Tkatch,[2] L. N. Uvarov,[2] A. A. Vorobyov,[2] Yan Jie,[3] Zhao Wenheng,[3] Zheng Shuchen,[3] and Zhong Yuanyuan,[3]

(E761 Collaboration)

[1] *Fermi National Accelerator Laboratory, Batavia, Illinois 60510*
[2] *Petersburg Nuclear Physics Institute, Gatchina, Russia*
[3] *Institute of High Energy Physics, Beijing, People's Republic of China*
[4] *H. H. Wills Physics Laboratory, University of Bristol, Bristol, United Kingdom*
[5] *Carnegie Mellon University, Pittsburgh, Pennsylvania 15213*
[6] *University of Iowa, Iowa City, Iowa 52242*
[7] *Institute of Theoretical and Experimental Physics, Moscow, Russia*
[8] *State University of New York at Albany, Albany, New York 12222*
[9] *Universidade Federal da Paraiba, Paraiba, Brazil*
[10] *Centro Brasileiro de Pesquisas Fisicas, Rio de Janeiro, Brazil*
[11] *Conselho Nacional de Pesquisas, Conselho Nacionale de Desenvolvimento Científico e Technológico, Rio de Janeiro, Brazil*
[12] *Universidade de Sao Paulo, Sao Paulo, Brazil*
[13] *J. W. Gibbs Laboratory, Yale University, New Haven, Connecticut 06511*

(Received 1 July 1993)

We have measured the branching ratio for the hyperon radiative decay $\Xi^- \to \Sigma^-\gamma$ from a sample of 211 ± 33 events obtained in the polarized 375 GeV/c charged hyperon beam at Fermilab. We find $B(\Xi^- \to \Sigma^-\gamma/\Xi^- \to \Lambda^0\pi^-) = (1.22 \pm 0.23 \pm 0.06) \times 10^{-4}$ where the quoted errors are statistical and systematic, respectively. We have also obtained an indication that the sign of the asymmetry parameter of this decay is positive.

PACS numbers: 13.40.Hq, 14.20.Jn

A great deal of interest has been shown in hyperon radiative decays over the past thirty years [1]. A study of these provides insight into nonleptonic electroweak phenomena. Theoretical models have been able to predict some of the observed decay rates, and/or asymmetries, but they have been largely unsuccessful in obtaining a unified picture of all the hyperon radiative decays. Of particular interest is the decay $\Xi^- \to \Sigma^-\gamma$. The only previous measurement [2] of the branching ratio gave the result $B(\Xi^- \to \Sigma^-\gamma/\Xi^- \to \Lambda^0\pi^-) = (2.3 \pm 1.0) \times 10^{-4}$ from a sample of 11 candidate events. Within the quark framework this value is significantly larger than expected from single-quark transitions [3], and it exceeds predictions based on penguin diagrams [4] by more than 2 orders of magnitude. Two-quark transitions, which are thought to be a dominant process in other radiative decays, should not contribute to the $\Xi^- \to \Sigma^-\gamma$ decay amplitude since there is no valence u quark to absorb the exchanged $W^{\pm}$. Predictions based on phenomenological models do somewhat better. The above experimental value is consistent with the unitarity lower bound of 1.0×10^{-4}, and it agrees with a model with two-particle intermediate states, which predicts a value of 1.7×10^{-4} [5]. A recent vector-meson dominance model [1] gives a reasonable fit to the existing experimental data. Clearly, more data would provide firmer guidance for model building.

Fermilab experiment 761 was designed to study the radiative decays of the Σ^+ and Ξ^- hyperons. We have recently reported results [6] on the $\Sigma^+ \to p\gamma$ asymmetry parameter. Here we discuss the observation of a clean $\Xi^- \to \Sigma^-\gamma$ signal and a higher statistics measurement of the branching ratio. We are also able to give an indication of the sign for the $\Xi^- \to \Sigma^-\gamma$ asymmetry parameter.

The experiment was located in the Proton Center beam line at Fermilab. The configuration of the apparatus, described briefly here, is shown in Fig. 1. For a more detailed description the reader is referred to Ref. [7]. The Ξ^- were produced (~ 1000/s) by the Tevatron's 800 GeV protons incident on a 1.0 interaction length Cu target at the entrance to the 3.4 T hyperon magnet. This magnet has a curved channel, which selects a 375 GeV/c

0031-9007/94/72(6)/808(4)$06.00

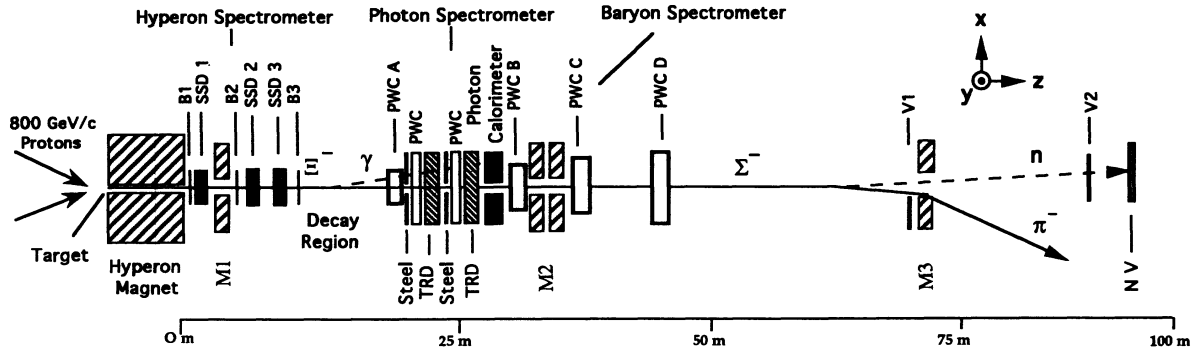

FIG. 1. Plan view of the E761 apparatus in the Fermilab Proton Center charged hyperon beam line.

secondary beam. The secondary beam was found to contain approximately 1% Ξ^- with the dominant component being π^-. The incident proton beam could be steered horizontally by upstream magnets to reverse the targeting angle which in turn reverses the vertical polarization vector of the produced Ξ^-.

Three spectrometers were used (Fig. 1), one each for the incident hyperon (Y), the decay baryon (B), and the photon, corresponding to the generic radiative decay $Y \to B\gamma$. The hyperon spectrometer consisted of 9 planes of 50 μm pitch silicon strip detectors in three stations (SSD 1-3), and a 2 m long magnet $M1$, which imparted a transverse momentum (ΔP_t) of -1.3 GeV/c. The baryon spectrometer included 30 planes of proportional wire chambers [24 (6) with 1 mm (2 mm) pitch], arranged in 4 stations (PWC A-D). Two dipole magnets (shown together as $M2$) connected in series provided a combined ΔP_t of 1.6 GeV/c to particles in the baryon spectrometer. The hyperon and baryon spectrometers had respective resolutions (1σ) in momentum, horizontal, and vertical angles of (0.8%, 12 μrad, 5 μrad) and (1.7%, 21 μrad, 12 μrad) at $p = 375$ GeV/c. A 12 m long decay region separated these two spectrometers. The photon spectrometer was located in the upstream end of the baryon spectrometer and was used to determine the position and energy of the photon. At the upstream end of this device there were two steel plates (each 1.44 radiation lengths thick) to convert photons. Each plate was followed by 2 PWC ($X+Y$) planes and 2 planes ($X+Y$) of transition radiation detectors (TRD) with 2 mm pitch to determine the position of the produced showers. At the downstream end a segmented lead glass/bismuth germanate (BGO) photon calorimeter was used to measure shower energy [$\Delta E(\text{GeV})/E \sim 30\%/\sqrt{E}$ plus a constant 3% added in quadrature], and its segmentation allowed for position measurements as well. A 76 × 76 mm^2 hole in the photon spectrometer, centered on the beam line, allowed the decay baryons and undecayed beam to pass through. The hole through the lead glass was lined with BGO crystals, which provided finer segmentation and greater energy confinement near the forward direction. Downstream of the baryon spectrometer a single dipole magnet $M3$ ($\Delta P_t = 0.7$ GeV/c) was used to separate neutrons and π^- that result from the decay sequence $\Xi^- \to \Sigma^-\gamma$, $\Sigma^- \to n\pi^-$.

Trigger conditions were imposed by scintillation counters in each of the spectrometers. Hyperon candidates were selected from the 180 kHz beam by requiring a single charged particle in the trigger counters $B1$–$B3$ during a 400 ns time window. A combination of scintillators before and after the steel plates of the photon spectrometer (not shown in Fig. 1) selected events in which at least one photon produced a shower in one of the steel plates. Two scintillator veto counters were placed downstream of the baryon spectrometer to reduce the trigger rate: The first $V1$ in front of magnet $M3$ vetoed events with low baryon momentum, while the second $V2$, 50 m downstream of the baryon spectrometer, eliminated very forward tracks from undecayed beam particles. A logical OR overrode the $V2$ veto if more than 2.5 GeV was deposited in the photon calorimeter. The final trigger rate was typically 1.0% of the beam rate. The geometrical acceptance of the apparatus and trigger for the $\Xi^- \to \Sigma^-\gamma$ decay within the decay region was $\sim 4\%$.

Data were collected over a 5 week period during the Fermilab 1990 fixed target run. A total of 2.8×10^8 triggers were recorded on magnetic tape with approximately equal samples taken at horizontal targeting angles (x-z plane; see Fig. 1) near ± 1.8 mrad. For the branching ratio calculation both samples were treated independently due to differences in beam phase space. All events were first analyzed for single tracks in the hyperon and baryon spectrometers, and a series of kinematic and fit quality cuts were applied. The missing mass squared (M_X^2) was then calculated based on the hypothesis $\Xi^- \to \Sigma^- X$. All events with $| M_X^2 | \leq 0.02$ GeV$^2/c^4$ were selected for further analysis. The 9.5×10^6 events selected in this range were well separated from the dominant decay channels of Σ^-, Ξ^-, and Ω^-. However, the decays $\overline{\Sigma}^- \to \bar{p}\pi^0$ and $K^- \to \pi^-\pi^0$ do fall in this range and completely mask any signal from $\Xi^- \to \Sigma^-\gamma$ without further selection.

We extracted the $\Xi^- \to \Sigma^-\gamma$ radiative decay signal

from the background in two stages. The first stage exploited the decay of the Σ^- daughter, $\Sigma^- \to n\pi^-$. Offline we extrapolated the trajectory of the baryon track into the 0.64 cm thick scintillator, NV (Fig. 1). If the baryon were indeed a Σ^- it would decay, and the resulting neutron would not produce a signal in the NV counter while the π^- would be swept away from the NV counter by the magnet $M3$. Assuming this to be true, a radiative decay candidate ought not to give a signal in the NV scintillator [8]. On the other hand, if the downstream baryon candidate (residual undecayed beam $\bar{p}$ from $\overline{\Sigma}^- \to \bar{p}\pi^0$, or a high momentum pion from K^- decay) did not decay it would produce a signal in NV. A position cut requiring the extrapolated baryon track to pass through the NV counter significantly reduced the background for selected events with no NV signal. The net result of this procedure was an increase in the signal-to-background ratio to about 1:7.

The second stage of the background elimination made use of the segmentation of the lead-glass/BGO calorimeter. The dimensions of the lead-glass blocks were 10 × 10 × 40 cm^3 and the BGO crystals, 2.5 × 2.5 × 20.0 cm^3. All but the front layer had the long dimension parallel to the beam. The high energy component of a shower from a single photon conversion is deposited along or near the original photon's path, whereas showers developed from background π^0 decays produce a broader pattern of energy deposition. From the measured hyperon and baryon tracks we extrapolated the missing neutral particle's trajectory into the photon calorimeter and determined the fraction of energy in the blocks or nearest neighbors along the trajectory. We required this energy fraction to be greater than 85% of the total energy in the photon calorimeter. This procedure increased the signal-to-background ratio to approximately 1:1. The result, shown in Fig. 2(a), clearly exhibits a peak at the photon mass based on the $\Xi^- \to \Sigma^-\gamma$ hypothesis. The dashed histogram is a Monte Carlo sample of $\overline{\Sigma}^- \to \bar{p}\pi^0$ events that do produce a signal in the NV counter but with otherwise the same cuts [9]. An alternative algorithm based on extrapolating the photon trajectory through the TRD-PWC system was also used, which yielded the result shown in Fig. 2(b) [7]. This result exhibits a cleaner signal but with fewer events in the signal peak due to the lower efficiency of this algorithm.

The branching ratio for $\Xi^- \to \Sigma^-\gamma$ decay is determined by comparing this decay mode with a sample of the dominant decay mode $\Xi^- \to \Lambda^0\pi^-$. The latter was obtained from a prescaled fraction of beam tracks collected with the regular trigger events. The branching ratio is given by

$$B\left(\frac{\Xi^- \to \Sigma^-\gamma}{\Xi^- \to \Lambda^0\pi^-}\right) = \left(\frac{N_\gamma}{\epsilon_\gamma}\right)\left(\frac{\epsilon_\Lambda}{N_\Lambda}\right)\left(\frac{1}{F}\right), \qquad (1)$$

where N_γ is the number of observed signal events obtained from the fits shown in Fig. 2, N_Λ is the number of events seen in the $\Xi^- \to \Lambda^0\pi^-$ normalization mode, ϵ_γ and ϵ_Λ are the detection efficiencies including trigger, acceptance, and cuts, and F is the prescale factor for the normalization signal. Because the reconstruction algorithm is sensitive to single charged tracks in the baryon spectrometer, the normalization signal is dominated by the neutral mode ($\Lambda^0 \to n\pi^0$) of the $\Xi^- \to \Lambda^0\pi^-$ decay. This provided events that were topologically similar to the radiative decay mode, which allowed for some cancelation of common terms in the efficiency calculations. The efficiencies were determined from Monte Carlo (MC) simulation of the experimental apparatus. The MC data were subjected to the same triggers and cuts as the experimental data. Corrections were included for trigger efficiencies from a study of the prescaled beam sample.

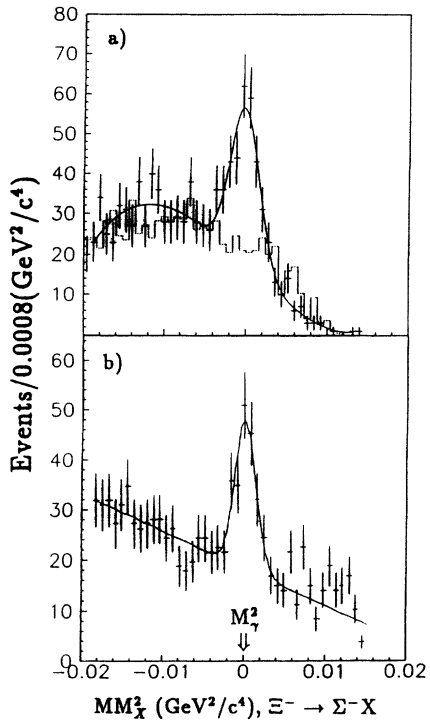

FIG. 2. Distribution of missing mass squared for the hypothesis $\Xi^- \to \Sigma^- X^0$: (a) For PbG/BGO analysis with energy fraction > 85%. Dashed line is Monte Carlo events for $\overline{\Sigma}^- \to \bar{p}\pi^0$ background. Solid line is best fit to signal plus background data. See text. (b) For TRD-PWC analysis.

Table I lists the values used in Eq. (1) and the calculated branching ratio for the two independent targeting angles. These data include only the results of the lead-glass analysis. A weighted average of the two values yields a final result for the $\Xi^- \to \Sigma^-\gamma$ branching ratio:

$$B\left(\frac{\Xi^- \to \Sigma^-\gamma}{\Xi^- \to \Lambda^0\pi^-}\right) = (1.22 \pm 0.23 \pm 0.06) \times 10^{-4}.$$

The first error is statistical and the second systematic. Similar results were obtained using the TRD-PWC anal-

TABLE I. Parameters used for branching ratio (B) in Eq. (1).

Tgt. ang.	+1.8 mrad	−1.8 mrad
N_γ	87 ± 22	124 ± 25
N_Λ	253 ± 46	559 ± 55
ϵ_γ	(0.59 ± 0.04) %	(0.71± 0.05) %
ϵ_Λ	(3.7 ± 0.1) %	(6.2 ± 0.1) %
F	16297 ± 24	16297 ± 24
B	$(1.32 \pm 0.42) \times 10^{-4}$	$(1.18 \pm 0.27) \times 10^{-4}$
B Weighted Avg.	$(1.22 \pm 0.23) \times 10^{-4}$	

ysis [$B = (1.44 \pm 0.37) \times 10^{-4}$] but with larger statistical errors. The dashed line in Fig. 2(a) is the MC predicted background shape. With this background shape a best fit to the data gives a 5% difference from that obtained from a third degree polynomial plus Gaussian fit to the data (solid line).

To study the systematics we first used the Monte Carlo simulation to determine how to divide the data into two samples containing approximately equal numbers of signal events. This was done for both the desired signal $\Xi^- \to \Sigma^-\gamma$ and the normalizing signal $\Xi^- \to \Lambda^0\pi^-$, and for each variable on which cuts were made. We then determined the branching ratio for the corresponding samples of real data. For details the reader is referred to Ref. [7]. The results of this study were consistent with the systematic error being completely dominated by the statistical error. The systematic uncertainty quoted above arises from the variation of the background shape used in the fitting procedure.

The above result is in agreement with the previously measured value [2]. We confirm, with significantly improved precision, that the $\Xi^- \to \Sigma^-\gamma$ branching ratio is an order of magnitude smaller than those of the other measured hyperon radiative decays, and it is very close to the unitarity lower bound of 1.0×10^{-4} [5].

Despite the small number of $\Xi^- \to \Sigma^-\gamma$ events, we attempted to obtain the asymmetry parameter (α_γ) for this decay. With horizontal targeting the polarization $\mathbf{P}$ of the Ξ^- is in the vertical ($\pm y$) direction. A bias-canceling procedure [6] was used to determine the asymmetry ($A_\gamma = \alpha_\gamma P$) from data taken at opposite targeting angles. We estimate a −11.0% polarization for the Ξ^- [10] and that the asymmetry for the events in Fig. 2 is a linear combination of A_γ and the asymmetry of the background events under the peak (A_{bgd}). The asymmetry of the background can then be determined from those events which had a signal in the NV counter, and thus α_γ can be calculated. We find the asymmetry parameter for $\Xi^- \to \Sigma^-\gamma$ to be $\alpha_\gamma = 1.0 \pm 1.3$ where the error is statistical only. This result gives weak evidence (63% probability) that the sign of the asymmetry parameter is positive.

We wish to thank the staffs of Fermilab and the Petersburg Nuclear Physics Institute for their assistance. The loan of the photon calorimeter lead glass from Rutgers University is gratefully acknowledged. This work is supported in part by the U.S. Department of Energy under Contracts No. DE-AC02-80ER10587, No. DE-AC02-76CH03000, No. DE-AC02-76ER03075, the Russian Academy of Sciences, and the U.K. Science and Engineering Research Council. I.F.A. was supported by FAPESP, Brazil. P.G. and J.R.P.M. were partially supported by FAPESP and CNPq, Brazil. A.M. was partially supported by CONACyT, Mexico.

* Present address: Santa Cruz Institute for Particle Physics, University of California, Santa Cruz, CA 95064.
† Present address: Fermilab, Batavia, IL 60510.
‡ Present address: Department of Physics, University of Maryland, College Park, MD 20747.
§ Present address: Universidade de Sao Paulo, Sao Paulo, Brazil.
‖ Present address: Superconducting Super Collider Laboratory, Dallas, TX 75237.
¶ Present address: Department of Physics, Stanford University, Stanford, CA 94309.

[1] P. Żenczykowski, Phys. Rev. D **40**, 2290 (1989); **44**, 1485 (1991). This paper contains a more complete list of theoretical references.
[2] S. F. Biagi *et al.*, Z. Phys. C **35**, 143 (1985).
[3] L. Bergström and P. Singer, Phys. Lett. **169B**, 297 (1986).
[4] J. O. Eeg, Z. Phys. C **21**, 253 (1984).
[5] Ya. I. Kogan and M. A. Shifman, Yad. Fiz. **38**, 1045 (1983) [Sov. J. Nucl. Phys. **38**, 628 (1983)].
[6] M. Foucher *et al.*, Phys. Rev. Lett. **68**, 3004 (1992). A different configuration of the apparatus was used in this phase of the experiment.
[7] T. Dubbs, Ph.D. thesis, University of Iowa, 1993 (unpublished).
[8] A finite number (∼ 5%) of neutrons from the secondary decay $\Sigma^- \to n\pi^-$ will produce a signal in the NV scintillator due to interactions, or np scattering. This has been included in the efficiency calculations.
[9] We have checked that the shape of the background is the same if the NV counter does not have a signal. However, the sample has much higher statistics if we model the events with a signal in the counter. The requirement that the baryon track must extrapolate into the NV counter effectively eliminates contamination from $K^- \to \pi^0\pi^-$ background.
[10] J. Duryea *et al.*, Phys. Rev. Lett. **67**, 1193 (1991).

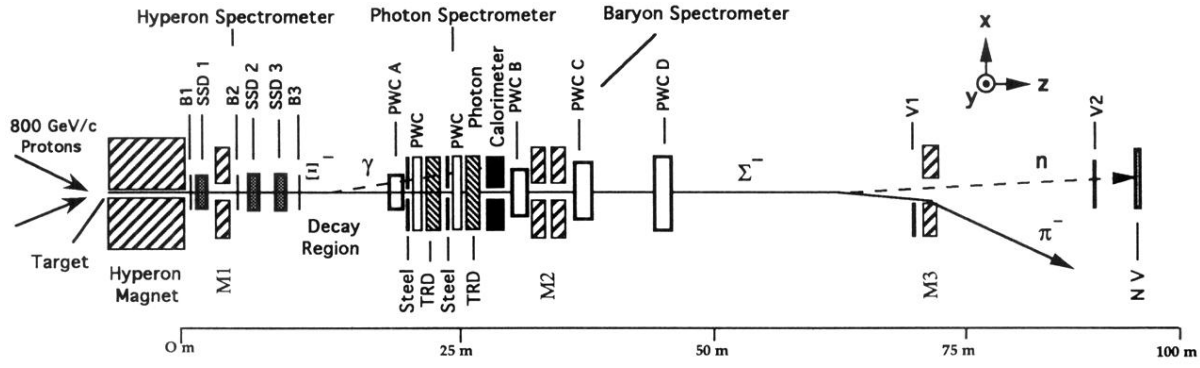

FIG. 1. Plan view of the E761 apparatus in the Fermilab Proton Center charged hyperon beam line.